



Chiral amorphous metal–organic polyhedra used as the stationary phase for high-resolution gas chromatography separations

Bo Tang | Chenyu Sun | Wei Wang | Lina Geng | Liquan Sun | Aiqin Luo

School of Life Science, Beijing Institute of Technology, Beijing, China

Correspondence

Aiqin Luo, School of Life Science, Beijing Institute of Technology,
No. 5 Zhongguancun South Street, Beijing 100081, China.
Email: aqluobit@163.com

Abstract

Herein, we describe a new chiral amorphous metal–organic polyhedra used as the stationary phase for high-resolution gas chromatography (GC). The chiral stationary phase was coated onto a capillary column via a dynamic coating process and investigated for a variety of compounds. The experimental results showed that the chiral stationary phase exhibits good selectivity for linear alkanes, linear alcohols, polycyclic aromatic hydrocarbons, isomers, and chiral compounds. In addition, the column has the advantages of high column efficiency and short analysis time. The present work indicated that amorphous metal–organic polyhedra have great potential for application as a new type of stationary phase for GC.

KEYWORDS

amorphous metal–organic polyhedra, chiral recognition, chiral stationary phases, gas chromatography

1 | INTRODUCTION

The separation and analysis of racemates are significant challenges in analytical chemistry.^{1–3} At present, the conventional method used for the analysis of racemates is chromatography, including high-performance liquid chromatography (HPLC), gas chromatography (GC), and capillary electrophoresis (CE).^{4–9} Furthermore, focus on the enantiomeric analysis obtained during chromatography has involved chiral stationary phases (CSPs). Although several commercial CSPs, such as cyclodextrin derivatives, have been widely used for the analysis of racemates in GC,^{10,11} there is still a need for the development of new CSPs with shorter analysis times or higher column efficiency and selectivity.

At present, porous solid materials (e.g., metal–organic frameworks [MOFs] and covalent-organic frameworks [COFs]) have been an active field of research in analytical chemistry.^{12–14} Because of their well-defined dimensions,

changeable pore size, and high surface area, these materials have been widely investigated due their potential application in gas storage, separation, and catalysis.^{15–20} Different from MOFs, metal–organic polyhedra (MOP) are a subclass of porous materials consisting of discrete coordination molecules. MOP materials have the advantage of being soluble in specific organic solvents and have the same potential applications as MOFs.^{21–23} For example, the application of crystalline MOPs in adsorption and separation has been researched.^{24–27} In addition to crystalline MOPs, amorphous MOP (aMOP) have also been prepared for many applications.^{28–30} For example, Gao et al. reported an amorphous metal–organic cage used to separate dye from water.²⁹ Although the packing of aMOP is random, the cages themselves will exist in cavities with defined sizes. Therefore, this type of material may also have good adsorption and separation performance. Inspired by this, we have prepared an aMOP solid and investigated its use as a stationary phase for GC

separations. As far as we know, this aMOP solid has not been used as a stationary phase for GC separation.

Herein, we report the use of a chiral amorphous MOP (aMOP-A) as the stationary phase for GC separations. Its separation performance was proven using alkanes, alcohols, esters, polycyclic aromatic hydrocarbons, phthalic esters, and enantiomers.

Enantiomers were separated on this column with excellent selectivity and reproducibility. The results demonstrated the broad application potential of aMOP-A as novel CSPs for GC separations.

2 | MATERIALS AND METHODS

2.1 | Chemicals and reagents

The 1,4,5,8-naphthalenetetracarboxylic dianhydride was purchased from Bide Pharmatech (China). L-Alanine, 2,6-lutidine, and $\text{Cu}(\text{NO}_3)_2 \cdot 3\text{H}_2\text{O}$ were purchased from Adamas-beta (China). *p*-Xylene was purchased from Aladdin (China). The remainder of the chemicals used in this study were purchased from Beijing Tongguang Fine (Beijing, China). All chemicals and solvents were used without further purification.

2.2 | Instrumentation

The untreated capillary column (0.25 mm, i.d. \times 20 m) was purchased from Ruifeng Chromatogram Apparatus Company. (Hebei, China). An Agilent 7890A (Palo Alto, USA) gas chromatograph equipped with a split/splitless injector and flame ionization detector (FID) was used for all GC separations. Powder X-ray diffraction (PXRD) data were collected on a Rigaku MiniFLEX 600 X-ray diffractometer using $\text{Cu K}\alpha$ radiation ($\lambda = 1.5406 \text{ \AA}$) in the 2θ range from 5° to 50° . A Thermo Scientific Nicolet iS5 Fourier transform infrared (FT-IR) spectrometer (Madison, USA) was used to obtain the FT-IR spectra of the sample using the KBr pellet method. Thermogravimetric analysis (TGA) was carried out on a Shimadzu DTG-60AH instrument (Kyoto, Japan) from room temperature to 500°C at a heating rate of $10^\circ\text{C min}^{-1}$ under a flow of nitrogen. Scanning electron microscopy (SEM) images were collected on a Phenom Pro scanning electron microscope (Holland) at 15 kV. The samples for SEM imaging were fixed on the sample stub using conductive double-coated carbon tape as an adhesive.

2.3 | Synthesis of aMOP-A

The ligand in aMOP-A (H_2L_A) was synthesized according to the method of Ghosh et al. with some modification.²¹

Typically, a mixture of 1,4,5,8-naphthalene tetracarboxylic dianhydride (2.679 g, 10.0 mmol) and L-alanine (1.783 g, 20.0 mmol) was added into 50 ml of acetic acid at 25°C and stirred at 100°C for 36 h. The resulting precipitate was filtered, washed with water, and dried at 60°C to give a brown solid (3.107 g, 76%).

The aMOP-A was synthesized according to the method of Ghosh et al. with some modification.²¹ Typically, a mixture of H_2L_A (0.4100 g, 1.0 mmol) and $\text{Cu}(\text{NO}_3)_2 \cdot 3\text{H}_2\text{O}$ (0.2416 g, 1.0 mmol) were dissolved in a mixed solution of *N,N*-dimethylformamide (DMF) (50 ml) and *p*-xylene (50 ml). The solution was stirred at 25°C for 1 h. Afterwards, 2,6-lutidine (1 ml) was added to the stirred suspension and the resulting mixture was stirred for 24 h. The resulting precipitate was filtered, washed with alcohol, and dried under vacuo at 100°C to give a green powder (0.4040 g, 62%).

2.4 | Preparation of the aMOP-A-coated capillary column

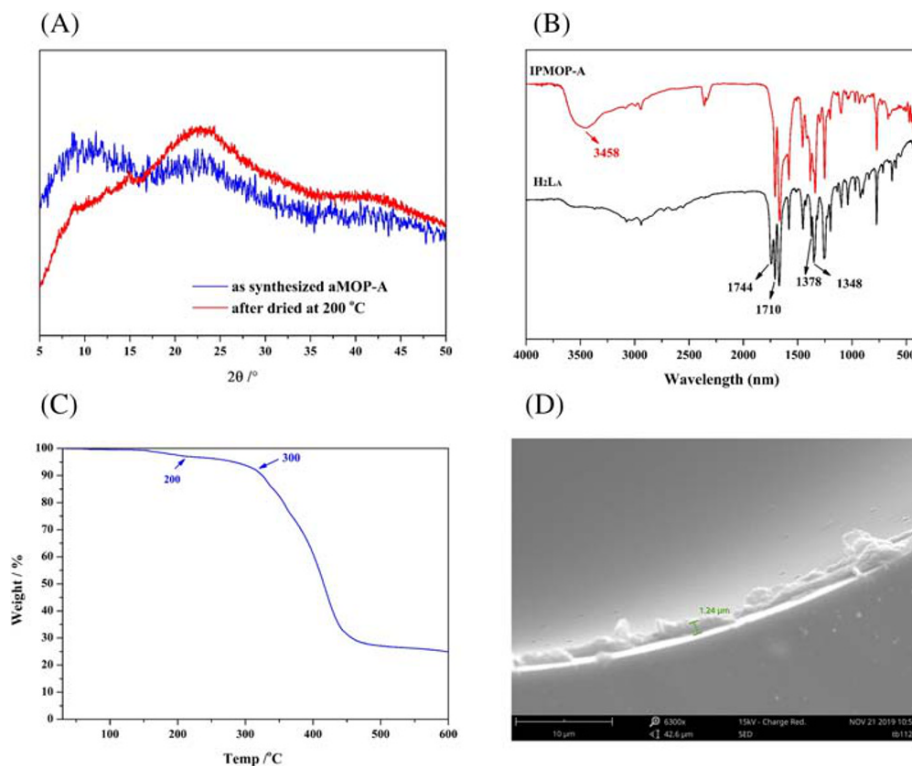
The capillary column (0.25 mm, i.d. \times 20 m long) was pretreated according to a literature procedure.^{31–33} First, the column was successively washed with 1 mol L^{-1} NaOH and ultrapure water and 0.1 mol L^{-1} HCl and ultrapure water. After the liquid flowed out of the capillary column, it was dried via a nitrogen purge at 200°C for 3 h.

A dynamic coating method was used to coat aMOP-A onto the pretreated capillary column.³⁴ Simply, 5 ml of an ethanol suspension of aMOP-A (2 mg ml^{-1}) was introduced into the pretreated capillary column under a N_2 gas pressure of 60 psi, keeping the gas pressure constant until all the liquid in the column flowed out. Last, the aMOP-A-coated column was purged for 6 h with N_2 in the temperature range from 40°C to 200°C .

2.5 | Derivatization of racemic compounds

The amino acid racemate was pretreated according to a literature procedure with some modifications.³¹ Briefly, 50-mg amino acid and 1 ml of isopropanol acetyl chloride (3/1, v/v) were added into a 10-ml pressure resistant reaction bottle and reacted for 30 min at 110°C , then dried under a flow of nitrogen gas, dissolved in 5 ml of tetrahydrofuran, reacted for 30 min at 100°C , dried under a flow of nitrogen gas, and dissolved in dichloromethane prior to use. The D- and L-isomers and racemates were prepared into their corresponding derivatives and were injected separately to determine the elution peak sequence.

FIGURE 1 (A) Powder X-ray diffraction (PXRD), (B) Fourier transform infrared (FT-IR), and (C) thermogravimetric analysis (TGA) curve obtained for aMOP-A. (D) Scanning electron microscopy (SEM) images of the cross-section of the chiral amorphous MOP (aMOP-A)-coated capillary column



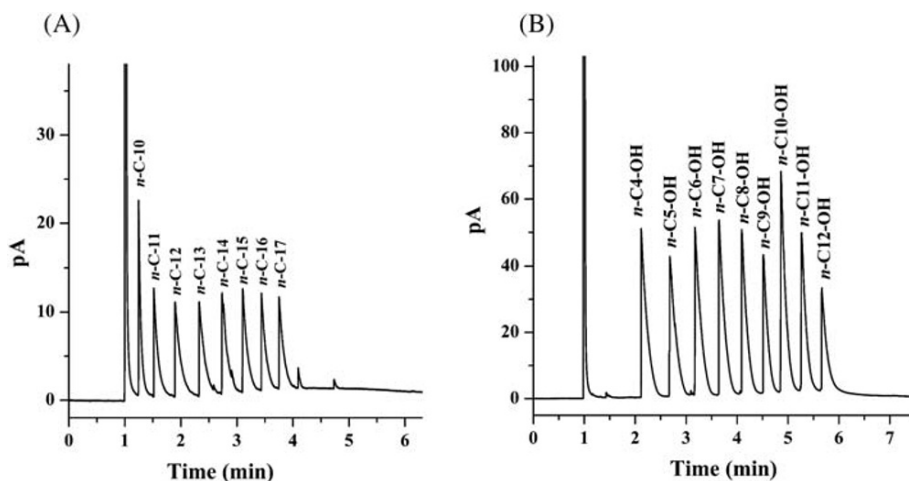
2.6 | Analysis conditions

Carrier gas, N₂ (99.999%); flow rate, 0.5 ml min⁻¹; oxidant gas, air (300 ml min⁻¹); fuel gas: H₂ (30 ml min⁻¹); split ratio, 50:1 (normally); detector temperature, 280°C; injection temperature, 260°C.

TABLE 1 McReynolds constants obtained for the chiral amorphous MOP (aMOP-A)-based stationary phase

X'	Y'	Z'	S'	U'	Average polarity
67	721.4	770.3	537.1	167.7	452.7

FIGURE 2 The separations of mixtures consisting of (A) linear alkanes and (B) normal alcohols on the chiral amorphous MOP (aMOP-A) capillary column. Temperature program: 60°C for 1.0 min, then heated to 150°C at 20°C min⁻¹; N₂ flow rate of 1.0 ml min⁻¹



3 | RESULTS AND DISCUSSION

3.1 | Characterization of the as-synthesized aMOP-A and aMOP-A-coated capillary column

PXRD confirmed that aMOP-A was an amorphous solid. Figure 1A shows the diffraction spectrum of aMOP-A, which displays only a few faint diffraction peaks signal, indicating that the solid was amorphous. After drying at 200°C, the diffraction pattern of aMOP-A showed no noticeable change, which indicates that the CSP can withstand high temperature. Figure 1B shows the FT-IR

spectra of H_2L_A and aMOP-A. For H_2L_A , the intense peaks observed at 1745 and 1378 cm^{-1} could be attributed to the stretching vibrations of C=O and C—O, respectively, whereas in aMOP-A, the peaks corresponding to C=O and C—O are red-shifted to 1710 and 1348 cm^{-1} , respectively, which may be due to the formation of Cu—O interactions. The strong band observed at 3458 cm^{-1} corresponded to the H_2O molecules in aMOP-A, which was consistent with the weight loss observed in TGA. TGA is often used to

characterize the thermal stability of CSPs. The TGA curves showed that aMOP-A was stable at temperatures below 300°C (Figure 1C). A weight loss of 4.0 wt.% was observed before 200°C , which was attributed to the loss of adsorbed water and guest solvents in aMOP-A. The experimental results showed that aMOP-A had good thermal stability and was a suitable material for use as a GC stationary phase. SEM is often used to characterize the microstructure of capillary columns. The column was truncated into $\sim 3\text{-mm}$

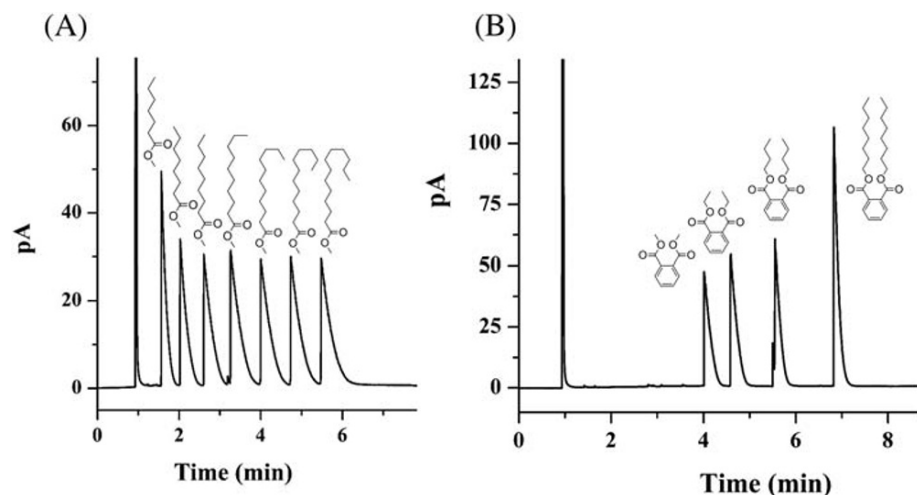


FIGURE 3 (A) The separation of a mixture of fatty acid ethyl esters (FAEEs). Peaks: (1) methyl caproate, (2) methyl enanthate, (3) methyl octanoate, (4) methyl nonoate, (5) methyl caprate, (6) methyl undecanate, and (7) methyl dodecylate. Temperature program: 90°C for 2.0 min, then heated to 160°C at $20^\circ\text{C min}^{-1}$. (B) The separation of phthalate acid esters (PAEs). Temperature program: 90°C for 1.0 min, then heated to 240°C at $20^\circ\text{C min}^{-1}$

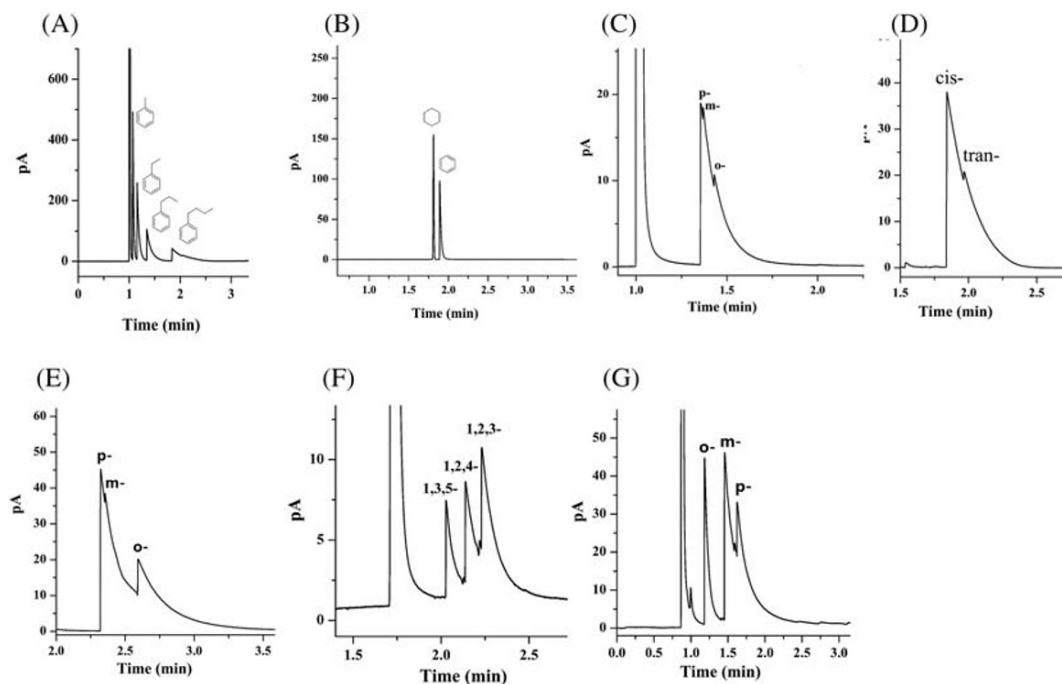


FIGURE 4 (A) The separation of a mixture of aromatic hydrocarbons. Peaks: (1) toluene, (2) ethylbenzene, (3) *n*-propylbenzene, and (4) *n*-butylbenzene. Temperature program: 50°C for 1.0 min, then heated to 150°C at $50^\circ\text{C min}^{-1}$; N_2 flow rate of 1.0 ml min^{-1} . (B) The separation of benzene and cyclohexane. Temperature program: 50°C , N_2 flow rate of 0.5 ml min^{-1} . (C) *o*-, *m*-, and *p*-xylene under 40°C . (D) (\pm)-Rose oxide at 110°C under a N_2 linear velocity of 0.8 ml min^{-1} . (E) *o*-, *m*-, and *p*-dichlorobenzene under 40°C . (F) 1,2,3-, 1,2,4-, and 1,3,5-trichlorobenzene. Temperature program: 65°C for 1.0 min, then heated to 100°C at $10^\circ\text{C min}^{-1}$. (G) *o*-, *m*-, and *p*-catechol. Temperature program: 120°C for 1.0 min, then heated to 150°C at $10^\circ\text{C min}^{-1}$

segments and fixed on the metal base to expose the cross-section inner wall for SEM.

The SEM images showed thin, solid films of aMOP-A (approximately 1.0 μm thick) were present on the inner walls of the capillary columns (Figure 1D). The images showed that the capillary columns were successfully prepared using aMOP-A as the stationary phase.

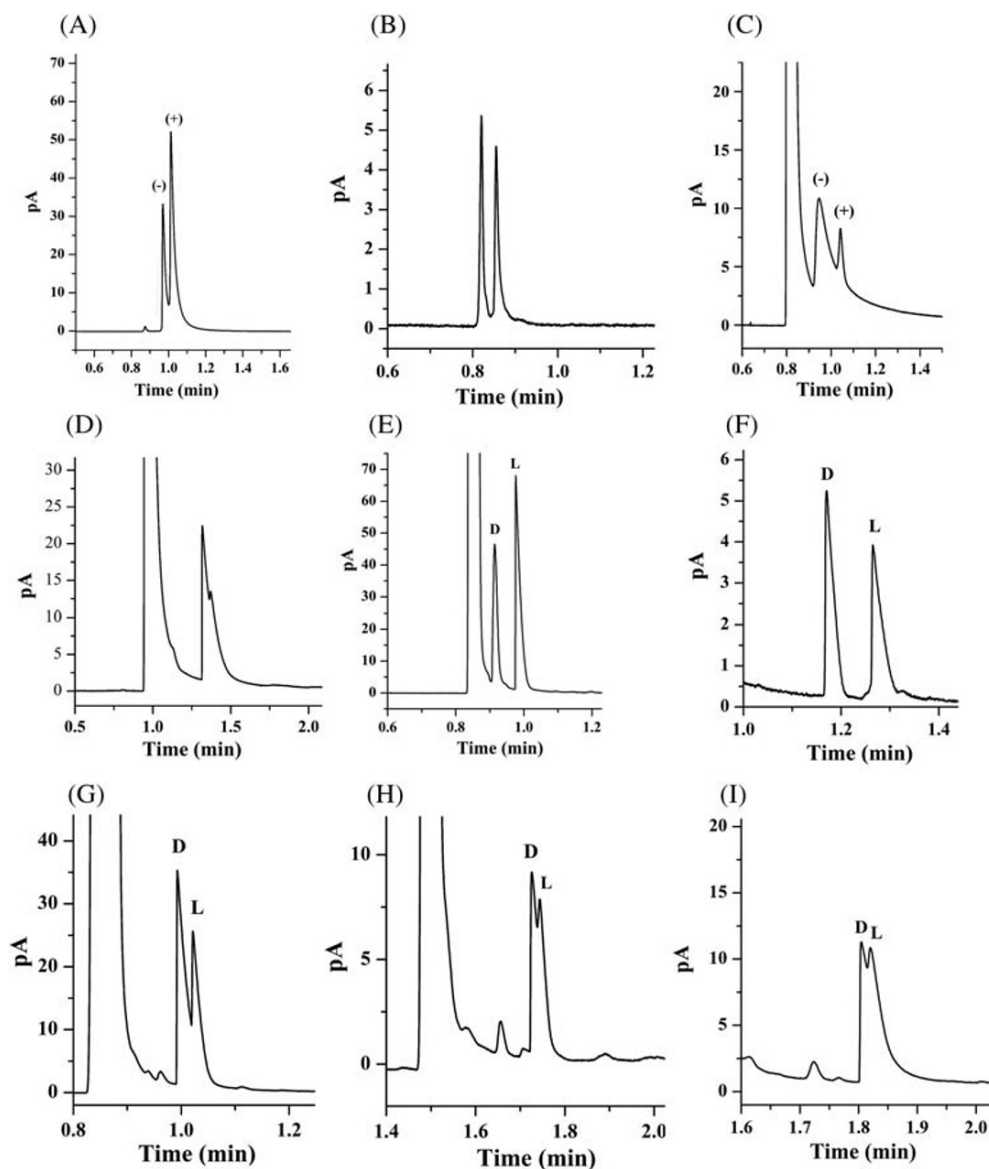
3.2 | Efficiency and McReynolds constants of the column

The column efficiency is an essential parameter to characterize the separation performance of a chromatographic column and is usually expressed by the number of theoretical plates. The chromatographic parameters of n -

dodecane were measured at 120°C to investigate the number of theoretical plates. The calculation results showed that the number of theoretical plates was found to be up to 4120 plates m^{-1} .

The McReynolds constant indicates the degree of attraction between the probe compound and the stationary phase, and it is generally characterized by the average polarity or general polarity.³² In this article, five probe compounds, benzene (X'), 1-butanol (Y'), 1-nitropropane (Z'), 2-pentanone (S'), and pyridine (U'), were selected to determine the McReynolds constants of the aMOP-A stationary phase. The average value of the five McReynolds constants obtained for aMOP-A was 452.7 (Table 1), indicating its high polarity. The elution order in this column for the five probe compounds was benzene, pyridine, 1-nitropropane, 1-butanol, and 2-pentanone.

FIGURE 5 Gas chromatography (GC) chromatograms obtained using the chiral amorphous MOP (aMOP-A)-coated capillary column during the separation of a variety of racemates. (A) Citronella at 130°C, (B) 1-(3-methylphenyl) ethanol at 160°C, (C) phenylsuccinic acid at 190°C, (D) *n*-butyl glycidyl ether at 75°C, (E) alanine derivative at 140°C, (F) glutamic derivative at 100°C, (G) lysine derivative at 120°C, and (H) tryptophan derivative at 140°C under a N_2 linear velocity of 0.5 ml min^{-1} . (I) Aspartic acid derivative at 135°C. The separation results are shown in Table 2



3.3 | Separation of alkane and alcohols mixture

A capillary column using aMOP-A as the stationary phase provided an appropriate resolution for the separation of linear alkane (Figure 2A) and normal alcohol (Figure 2B) mixtures. The aMOP-A-coated capillary column exhibited high-resolution performance during the separation of linear alkanes and normal alcohols. All analytes achieved baseline resolution, and their elution sequence was based on their boiling point (carbon number). Its significant high-resolution performance could be attributed to the synergistic effect of its multiple molecular interactions including van der Waals interactions and H-bonding.³¹

3.4 | Separation of FAEEs and PAEs

The aMOP-A-based capillary column showed excellent separation performance for nine fatty acid ethyl esters (FAEEs) mixtures. All the FAEEs achieved baseline separation, and the elution sequence was in accordance with their boiling points (Figure 3A).

Phthalate acid esters (PAEs) are the most common plasticizers. However, they have recently caused widespread public concern due to their carcinogenic and estrogenic properties. Figure 3B shows the aMOP-A-based capillary column achieved baseline separation for four PAEs, indicating that the aMOP-A column resulted in the good separation of the plasticizer and could adapt to the analysis of high boiling point materials.

3.5 | Separation of aromatic hydrocarbons and positional isomers

Figure 4A presents the separation results obtained for a mixture of four aromatic hydrocarbons (methylbenzene, ethylbenzene, *n*-propylbenzene, and *n*-butylbenzene) on

TABLE 2 The separation of various racemates on the chiral amorphous MOP (aMOP-A) capillary column

Racemate	<i>T</i> (°C)	<i>k</i>	α
Citronella	130	0.73	1.05
1-(3-Methylphenyl)ethanol	160	0.45	1.04
Phenylsuccinic acid	190	0.77	1.11
<i>n</i> -Butyl glycidyl ether	75	1.34	1.05
Alanine ^a	140	0.66	1.07
Glutamic acid ^a	100	1.15	1.08
Lysine ^a	120	0.74	1.03
Tryptophan ^a	140	1.97	1.01
Aspartic acid ^a	135	2.10	1.01

^aTrifluoroacetyl isopropyl ester derivative.

the aMOP-A-coated capillary column. The four aromatic hydrocarbons were baseline separated on the aMOP-A-coated capillary column and eluted in the order of their boiling point. Benzene and cyclohexane have similar physical properties, so their separation is one of the most challenging tasks in the petrochemical industry.³⁵ Figure 4B shows a mixture of cyclohexane (b.p. 80.7°C) and benzene (b.p. 80.1°C) can be baseline separated on the aMOP-A column. However, they did not elute in the order of their boiling points. The separation efficiency of the pair on the aMOP-A column was mainly attributed to the molecular sieving effect between benzene and the aMOP stationary phase.^{31,36}

We also tested the resolving ability of the aMOP-A column to positional isomers. Figure 4C–G shows that the aMOP-A-coated capillary column also provided selectivity toward some mixtures of cis-trans isomers and positional isomers. The separation of positional isomers did not strictly comply with the order of their boiling points, which may be attributed to the molecular sieve effect of the CSP.

3.6 | Separation of racemates

We tested the chiral recognition capability of the capillary column using several compounds. The following 10 racemates were separated on the capillary column:

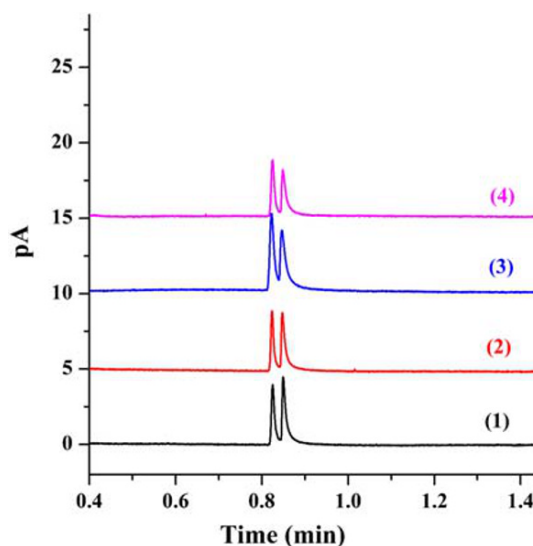


FIGURE 6 Reproducible chromatograms obtained using the chiral amorphous MOP (aMOP-A)-coated capillary column for the separation of 1-(3-methylphenyl)ethanol at 160°C under a N₂ linear velocity of 1.0 ml min⁻¹. (1) The chromatogram obtained before the column was used for the separations. (2)–(4) The chromatograms obtained after the chiral column was subjected to 50, 100, and more than 200 injections

TABLE 3 Reproducibility and stability for the separations of the 1-(3-methylphenyl)ethanol on the chiral amorphous MOP (aMOP-A) capillary column

Analytes	Run-to-run ^d				Day-to-day ^d				Column-to-column ^d			
	<i>K</i> ^b	RSD (%)	<i>N</i> ^c	RSD (%)	<i>K</i> ^b	RSD (%)	<i>N</i> ^c	RSD (%)	<i>K</i> ^b	RSD (%)	<i>N</i> ^c	RSD (%)
1 ^a	0.40	0.49	4230	2.43	0.39	0.74	4,769	1.15	0.39	0.89	4,878	5.28
2 ^a	0.44	0.67	3765	1.25	0.44	0.67	3,216	4.08	0.43	1.17	2,544	7.49

^aChromatographic peak of 1-(3-methylphenyl)ethanol isomer.

^bRetention factor.

^cColumn efficiency.

^d*n* = 3 for test.

citronella, 1-(3-methylphenyl)ethanol, phenylsuccinic acid, *n*-butyl glycidyl ether, alanine derivative, glutamic acid derivative, lysine derivative, tryptophan derivative, and aspartic acid derivative. Figure 5 shows the column had an appropriate resolution and short retention time for racemates. Citronella, 1-(3-methyl phenyl) ethanol, alanine derivative, and glutamic acid derivative achieved baseline separation (Table 2). The results showed that the aMOP-A capillary column was suitable for the separation of a variety of amino acid racemates in GC. The chiral recognition ability of the aMOP-A-coated column could be attributed to the existence of the chiral microenvironment in the cavities of aMOP-A. Although aMOP-A was amorphous and randomly distributed in the column, the cavities in aMOP-A had regular size and shape, which provided the columns chiral recognition capability. Besides, many other interactions, including H-bonding, inductive forces, and dispersion forces, also affected the chiral identification process in GC.

3.7 | Column reproducibility and stability

The reproducibility and stability of the aMOP-A-coated column were also explored. Under the same chromatographic conditions, we repeatedly injected samples to test the chromatograms of 1-(3-methylphenyl)ethanol. The chromatograms are shown in Figure 6. The chromatograms showing the elution times after 50, 100, and 200 injections had no significant difference. Table 3 provides the *k* (retention factor) and *N* (efficiency) results with the RSD values of 0.49–1.17% and 1.15–7.49% for 1-(3-methylphenyl)ethanol, proving its good stability on its separation performance. This indicated that there was no significant change in the enantioselectivity and recognition ability of the column after multiple injections. The results also indicated that this novel CSP for GC was extremely stable. The good repeatability and stability of the aMOP-A-coated column demonstrated its potential practical application.

4 | CONCLUSIONS

In conclusion, we have prepared a new aMOP-A and studied its potential use as a CSP in GC. The aMOP-A-coated capillary column displayed excellent selectivity during the separation of hydrocarbons, alcohols, PAEs, FAEEs, isomers, and racemates. In addition, the aMOP-A-coated column exhibited high column efficiency and short analysis times. Although the preparation and separation mechanism of aMOP has yet to be studied, we believe that aMOP as a novel CSP has great potential application in GC separations.

ORCID

Aiqin Luo  <https://orcid.org/0000-0001-6558-6696>

REFERENCES

- Xie SM, Zhang ZJ, Wang ZY, Yuan LM. Chiral metal-organic frameworks for high-resolution gas chromatographic separations. *J Am Chem Soc.* 2011;133(31):11892-11895.
- Boer SA, Nolvachai Y, Kulsing C, et al. Liquid-phase enantioselective chromatographic resolution using interpenetrated, homochiral framework materials. *Chem. A Eur. J.* 2014;20:11308-11312.
- De Camp WH. Chiral drugs: the FDA perspective on manufacturing and control. *J Pharm Biomed Anal.* 1993;11(11-12):1167-1172.
- Zhang JH, Xie SM, Wang BJ, He PG, Yuan LM. A homochiral porous organic cage with large cavity and pore windows for the efficient gas chromatography separation of enantiomers and positional isomers. *J Sep Sci.* 2018;41(6):1385-1394.
- Li YX, Fu SG, Zhang JH, et al. A highly ordered chiral inorganic mesoporous material used as stationary phase for high-resolution gas chromatographic separations. *J Chromatogr a.* 2018;1557:99-106.
- Zhang M, Xue XD, Zhang JH, Xie SM, Zhang Y, Yuan LM. Enantioselective chromatographic resolution using a homochiral metal-organic framework in HPLC. *Anal Methods.* 2014; 6(2):341-346.
- Kuang X, Ma Y, Su H, Zhang J, Dong YB, Tang B. High-performance liquid chromatographic enantioseparation of racemic drugs based on homochiral metal-organic framework. *Anal Chem.* 2014;86(2):1277-1281.

8. Fei ZX, Zhang M, Zhang JH, Yuan LM. Chiral metal-organic framework used as stationary phases for capillary electrochromatography. *Anal Chim Acta*. 2014;830:49-55.
9. Okamoto Y, Ikai T. Chiral HPLC for efficient resolution of enantiomers. *Chem Soc Rev*. 2008;37(12):2593-2608.
10. Xie SM, Chen XX, Zhang JH, Yuan LM. Gas chromatographic separation of enantiomers on novel chiral stationary phases. *TrAC Trends Anal Chem*. 2020;124:115808.
11. Zhang JH, Xie SM, Zi M, Yuan LM. Recent advances of application of porous molecular cages for enantioselective recognition and separation. *J Sep Sci*. 2020;43(1):134-149.
12. Ehrling S, Kutzscher C, Freund P, Müller P, Senkovska I, Kaskel S. MOF@SiO₂core-shell composites as stationary phase in high performance liquid chromatography. *Microporous Mesoporous Mater*. 2018;263:268-274.
13. Tang WQ, Xu JY, Gu ZY. Metal-organic-framework-based gas chromatographic separation. *Chem - an Asian J*. 2019;14(20):3462-3473.
14. Ma YX, Li ZJ, Wei L, Ding SY, Zhang YB, Wang W. A dynamic three-dimensional covalent organic framework. *J Am Chem Soc*. 2017;139(14):4995-4998.
15. Xue DX, Wang Q, Bai J. Amide-functionalized metal-organic frameworks: syntheses, structures and improved gas storage and separation properties. *Coord Chem Rev*. 2019;378:2-16.
16. Petit C. Present and future of MOF research in the field of adsorption and molecular separation. *Curr Opin Chem Eng*. 2018;20:132-142.
17. Zhang Y, Feng X, Yuan S, Zhou J, Wang B. Challenges and recent advances in MOF-polymer composite membranes for gas separation. *Inorg Chem Front*. 2016;3(7):896-909.
18. Fu J, Das S, Xing G, Ben T, Valtchev V, Qiu S. Fabrication of COF-MOF composite membranes and their highly selective separation of H₂/CO₂. *J Am Chem Soc*. 2016;138(24):7673-7680.
19. Al-Rowaili FN, Jamal A, Ba Shammakh MS, Rana A. A review on recent advances for electrochemical reduction of carbon dioxide to methanol using metal-organic framework (MOF) and non-MOF catalysts: challenges and future prospects. *ACS Sustain Chem Eng*. 2018;6(12):15895-15914.
20. Han AJ, Wang BQ, Kumar A, et al. Recent advances for MOF-derived carbon-supported single-atom catalysts. *Small Methods*. 2019;3(9):1800471.
21. Mollick S, Mukherjee S, Kim D, et al. Hydrophobic shielding of outer surface: enhancing the chemical stability of metal-organic polyhedra. *Angew Chemie - Int Ed*. 2019;58(4):1041-1045.
22. Fulong CRP, Liu J, Pastore VJ, Lin H, Cook TR. Mixed-matrix materials using metal-organic polyhedra with enhanced compatibility for membrane gas separation. *Dalt Trans*. 2018;47(24):7905-7915.
23. Vardhan H, Yusubov M, Verpoort F. Self-assembled metal-organic polyhedra: an overview of various applications. *Coord Chem Rev*. 2016;306:171-194.
24. Chen L, Yang T, Cui H, Cai T, Zhang L, Su CY. A porous metal-organic cage constructed from dirhodium paddle-wheels: synthesis, structure and catalysis. *J Mater Chem a*. 2015;3(40):20201-20209.
25. Zou Y, Park M, Hong S, Lah MS. A designed metal-organic framework based on a metal-organic polyhedron. *Chem Commun*. 2008;(20):2340-2342.
26. Li JR, Yu J, Lu W, et al. Porous materials with pre-designed single-molecule traps for CO₂ selective adsorption. *Nat Commun*. 2013;4(1):1538.
27. Jaya Prakash M, Oh M, Liu XF, Han KN, Seong GH, Lah MS. Edge-directed [(M₂)₂L₄] tetragonal metal-organic polyhedra decorated using a square paddle-wheel secondary building unit. *Chem Commun*. 2010;46(12):2049-2051.
28. Li ZY, Zhang Y, Zhang CW, et al. Cross-linked supramolecular polymer gels constructed from discrete multi-pillar[5]arene metallacycles and their multiple stimuli-responsive behavior. *J Am Chem Soc*. 2014;136(24):8577-8589.
29. Gao Y, Deng SQ, Jin X, Cai SL, Zheng SR, Zhang WG. The construction of amorphous metal-organic cage-based solid for rapid dye adsorption and time-dependent dye separation from water. *Chem Eng J*. 2019;357:129-139.
30. Jin X, Zhang YP, Li DM, et al. The interaction of an amorphous metal-organic cage-based solid (aMOC) with miRNA/DNA and its application on a quartz crystal microbalance (QCM) sensor. *Chem Commun*. 2020;56(4):591-594.
31. Chang N, Gu ZY, Yan XP. Zeolitic Imidazolate framework-8 nanocrystal coated capillary for molecular sieving of branched alkanes from linear alkanes along with high-resolution chromatographic separation of linear alkanes. *J Am Chem Soc*. 2010;132(39):13645-13647.
32. Yu L, He J, Qi ML, Huang XB. Amphiphilic triptycene-based stationary phase for high-resolution gas chromatographic separations. *J Chromatogr A*. 2019;1599:239-246.
33. He J, Yu L, Huang X, Qi ML. Triptycene-based stationary phases for gas chromatographic separations of positional isomers. *J Chromatogr a*. 2019;1599:223-230.
34. Fang ZL, Zheng SR, Tan JB, et al. Tubular metal-organic framework-based capillary gas chromatography column for separation of alkanes and aromatic positional isomers. *J Chromatogr A*. 2013;1285:132-138.
35. Cui Y, Yao H, Yang C, Yan X. In situ fabrication of microporous organic network coated capillary column for high resolution gas chromatographic separation of hydrocarbons. *Electrophoresis*. 2019;40(16-17):2186-2192.
36. Clever GH, Punt P. Cation-anion arrangement patterns in self-assembled Pd₂L₄ and Pd₄L₈ coordination cages. *Acc Chem Res*. 2017;50(9):2233-2243.

How to cite this article: Tang B, Sun C, Wang W, Geng L, Sun L, Luo A. Chiral amorphous metal-organic polyhedra used as the stationary phase for high-resolution gas chromatography separations. *Chirality*. 2020;1-8. <https://doi.org/10.1002/chir.23263>